Journal of Disability Research

2023 | Volume 2 | Issue 2 | Pages: 79–88
DOI: 10.57197/JDR-2023-0023

# Optimal Deep Recurrent Neural Networks for IoT-enabled Human Activity Recognition in Elderly and Disabled Persons

Faiz Alotaibi[1,2], Mrim M. Alnfiai[2,3,*], Fahd N. Al-Wesabi[4], Mesfer Alduhayyem[5], Anwer Mustafa Hilal[6] and Manar Ahmed Hamza[6]

[1]Department of Information Science, College of Arts, King Saud University, Riyadh, Saudi Arabia
[2]King Salman Center for Disability Research, Riyadh, Saudi Arabia
[3]Department of Information Technology, College of Computers and Information Technology, Taif University, Taif 21944, Saudi Arabia
[4]Department of Computer Science, College of Science and Art at Mahayil, King Khalid University, Saudi Arabia
[5]Department of Computer Science, College of Computer Engineering and Sciences, Prince Sattam Bin Abdulaziz University, Al-Kharj 16273, Saudi Arabia
[6]Department of Computer and Self Development, Preparatory Year Deanship, Prince Sattam Bin Abdulaziz University, Al-Kharj, Saudi Arabia

Correspondence to:
Mrim M. Alnfiai*, e-mail: m.alnofiee@tu.edu.sa

Received: May 11 2023; Revised: July 18 2023; Accepted: July 20 2023; Published Online: August 18 2023

## ABSTRACT

Aging is related to a decrease in the ability to execute activities of day-to-day routine and decay in physical exercise, which affect mental and physical health. Elderly patients or people can depend on a human activity recognition (HAR) system, which monitors the activity interventions and patterns if any critical event or behavioral changes occur. A HAR system incorporated with the Internet of Things (IoT) environment might allow these people to live independently. While the number of groups of activities and sensor measurements is enormous, the HAR problem could not be resolved deterministically. Hence, machine learning (ML) algorithm was broadly applied for the advancement of the HAR system to find the patterns of human activity from the sensor data. Therefore, this study presents an Optimal Deep Recurrent Neural Networks for Human Activity Recognition (ODRNN-HAR) on Elderly and Disabled Persons technique in the IoT platform. The intension of the ODRNN-HAR approach lies in the recognition and classification of various kinds of human activities in the IoT environment. Primarily, the ODRNN-HAR technique enables IoT devices to collect human activity data and employs *Z*-score normalization as a preprocessing step. For effectual recognition of human activities, the ODRNN-HAR technique uses the DRNN model. At the final stage, the optimal hyperparameter adjustment of the DRNN model takes place using the mayfly optimization (MFO) algorithm. The result analysis of the ODRNN-HAR algorithm takes place on benchmark HAR dataset, and the outcomes are examined. The comprehensive simulation outcomes highlighted the improved recognition results of the ODRNN-HAR approach in terms of different measures.

## KEYWORDS

human activity recognition, Internet of Things, deep recurrent neural network, mayfly optimization, disabled persons

## INTRODUCTION

The automated services presented to an aging population to help them live healthily and independently in their houses have paved the way for a new field of economics (Shan et al., 2020). With advancements in the Internet of Things (IoT), the smart home is the solution to offer home services, like energy management, security, healthcare monitoring, and assistance in daily tasks (Ullah et al., 2019). A smart home can be equipped with numerous actuators and sensors that could identify their temperature and humidity, opening of doors, the room's luminosity, etc. Also, it controls few instruments like household appliances, heating, lights, shutters, etc. (Li et al., 2021). Today, a lot of these devices are connected and controlled from a distance. Nowadays, washing machines, televisions, and refrigerators are found in houses called intelligent that have sensors and are controlled remotely (Rashid and Louis, 2019). Every gadget, object, sensor, and actuator can be interlinked using transmission protocols.

To render all these services, a smart home should recognize and understand the resident's actions (Zhang et al., 2020). Hence, scholars are devising methods of human activity recognition (HAR) that analyze and monitor the behavior of one or a few individuals to infer the activity that takes place (Brishtel et al., 2023). Commonly, HAR includes four stages: the user interface for the management of HAR, capturing of signal activity, artificial intelligence (AI)-based activity recognition, and data preprocessing. All stages are applied with many methods bringing the HAR system to many choices (Tang et al., 2021). Hence, the processes of AI techniques for activity detection, an optimum application domain, and the kind of data acquisition devices make the choices more challenging. Various studies implemented machine learning (ML) approaches in HAR (Li et al., 2019). They highly depend on feature extraction approaches, which include symbolic representation, time-frequency transformation, and statistical approaches. But the features abstracted are heuristic and carefully engineered. There were no systematic or universal feature extraction methods to capture differentiable features efficiently for HAR (Lattanzi et al., 2022). Currently, DL has embraced prominent success in devising higher-level abstractions from complex data in several areas like speech processing, natural language processing, and computer vision. Along with the remarkable growth of DL in HAR, latest studies are being undertaken to solve the particular difficulties (Qian et al., 2021).

This study presents an Optimal Deep Recurrent Neural Networks for Human Activity Recognition (ODRNN-HAR) on Elderly and Disabled Persons technique in IoT environment. The goal of the ODRNN-HAR method lies in the recognition and classification of various kinds of human activities in IoT environment. Primarily, the ODRNN-HAR technique enables IoT devices to collect human activity data and employs *Z*-score normalization as a preprocessing step. For effectual recognition of human activities, the ODRNN-HAR technique uses the DRNN model. At the final stage, the optimal hyperparameter adjustment of the DRNN model takes place using the mayfly optimization (MFO) algorithm. The result analysis of the ODRNN-HAR method takes place on benchmark HAR dataset, and the outcomes are examined in terms of different measures.

# RELATED STUDIES

In Park et al. (2023), the authors devised a DL-related HAR approach named MultiCNN-FilterLSTM that combined a multihead CNN with an LSTM using a residual connection where feature vectors are productively dealt with hierarchically. Consequently, a new method, filterwise LSTM (FilterLSTM), was presented that uses LSTM cells. Xu et al. (2020) modeled two improved HAR approaches related to deep CNN and Gramian angular field (GAF). First, the GAF method can be utilized for transforming the 1D sensor data as 2D images. After using the multi-dilated kernel residual module (Mdk-Res), a novel enhanced DCNN network Mdk-ResNet extracted the attributes among sampling points with various intervals. In Gumaei et al. (2019), a potential multi-sensors-related architecture was devised for HAR exploiting a hybrid DL algorithm that combined the GRUs with the simple recurrent unit of NNs. Also, the authors used the deep GRUs for examining instability or fluctuations in precision and vanishing gradient problems.

Islam et al. (2023) modeled a new DL-based approach STC-NLSTMNet abbreviated as spatio-temporal convolution with nested LSTM, with the capability to derive temporal and spatial features automatically and concurrently detect human action with more precision. The presented method has depth-wise separable convolution (DS-Conv) blocks, NLSTM, and feature attention module. In Anagnostis et al. (2021), they modeled a data gathered field experiment that extract information from 20 healthy participants utilizing five wearable sensors (gyroscopes, magnetometers, and entrenched with tri-axial accelerometers) linked to them. Concurrently, the gathered signals from on-body sensors are managed to remove noise and provide an LSTM-NN that can be broadly utilized in DL for recognizing features in time-dependent dataset series. Xia et al. (2020) modeled a structure that collected the raw data by mobile sensors that can be provided as 2-layer LSTM and then convolution layers. Moreover, a global average pooling layer has been implemented for replacing the FC layer and then convolutional to decrease model variables.

Dahou et al. (2022) propose a new HAR technique dependent upon optimizer 2 approaches like CNN and Arithmetic Optimization Algorithm (AOA) for boosting the HAR efficiency. The presented CNN was carried out for learning and extracting features in input data, but improved AOA technique termed Binary AOA (BAOA). Eventually, the SVM was implemented for classifying the chosen feature dependent upon distinct actions. In Mekruksavanich et al. (2020), the authors present a hybrid DL technique termed CNN-LSTM, which utilized LSTM for HAR with CNN. This method employs HAR containing smartwatches for categorizing hand activities. This technique utilized the Wireless Sensor Data Mining database.

# THE PROPOSED MODEL

This article presents an automatic HAR detection method using the ODRNN-HAR approach in IoT environment. The major intention of the ODRNN-HAR approach lies in the automated recognition and classification of various kinds of human activities in an IoT environment. In the presented MER-ODLADT technique, several subprocesses are involved, namely data preprocessing, DRNN-based activity recognition, and MFO-based hyperparameter tuning. Figure 1 illustrates the workflow of the ODRNN-HAR algorithm.

## Data normalization

Data normalization has been suitable for classifier problems as it proposes similar weight for every feature (Eskandari et al., 2023). There are three important approaches to data normalization comprising Normalization by decimal scaling, *Z*-score Normalization, and Min-Max Normalization. During this case, the Min-Max Normalization was exploited as it preserves the connection in the original database and carries out a linear transformation on the original database.

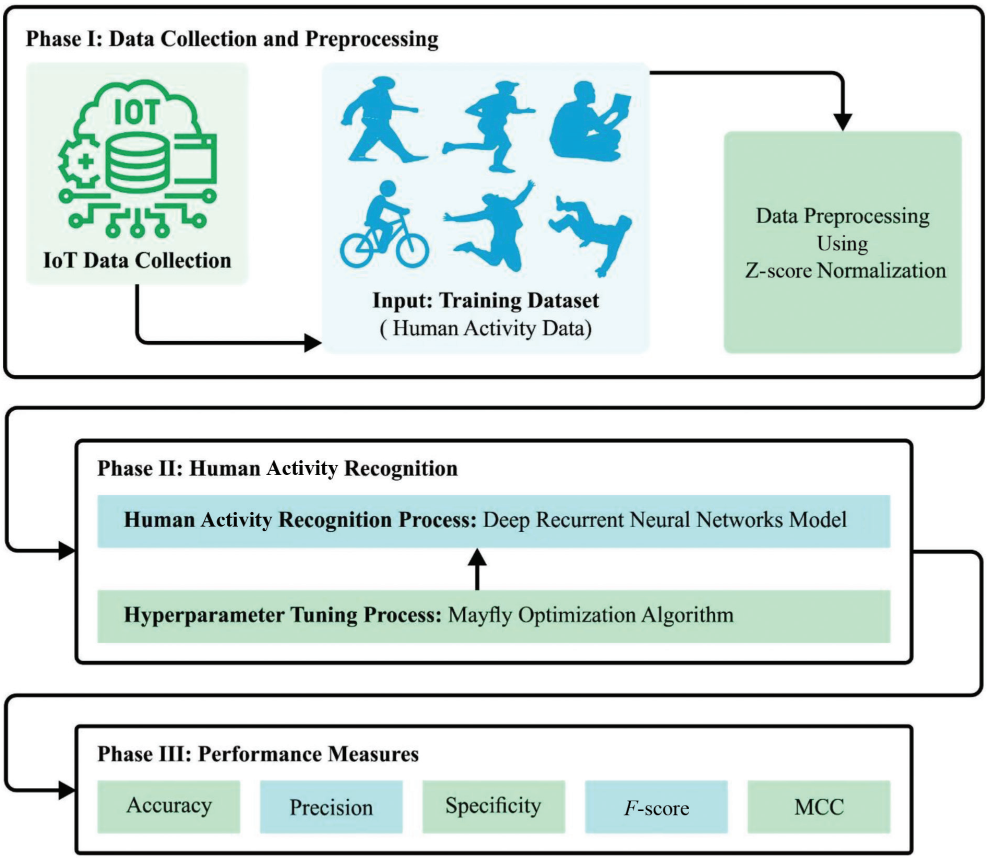


**Figure 1:** Workflow of the ODRNN-HAR algorithm. Abbreviations: IoT, Internet of Things; ODRNN-HAR, Optimal Deep Recurrent Neural Networks for Human Activity Recognition.

This approach converts the data as existing boundaries. The data are normalization from the range of 0 and 1 using Eq. (1):

$$x' = \frac{x - \min_Y}{\max_Y - \min_Y}, \tag{1}$$

where $x$ refers to the original value of feature $Y$, $x$' represents its normalization value, and $\max_Y$ and $\min_Y$ denote the maximal and minimal feature values of Y.

## Automated activity recognition using the DRNN model

To proficiently recognize and classify human activities, the DRNN model is applied. A persistent challenge with CNN is that they could not depict the temporal dependency in the operational dataset (Taheri et al., 2021). However, RNNs could preserve and utilize data across dissimilar time horizons during learning. A recursive structure enables RNN to retain the potential data of prior time step for additional prediction. Figure 2 shows the infrastructure of RNN.

Now, the RNN must forecast the normal or faulty outcomes of instances from the dataset based on the relationships between the output vector (d) and the input vector (X) calculated using the activation function (a). Usually, the input data combine measurements collected from weather-related features like mixed, supply, return, and outdoor air temperatures, the equipment's temperature set points, and a concatenation of operational variables like recorded signals. But typical RNNs do not embed long-term temporal dependency due to a problem known as the gradient vanishing problem. LSTM unit is integrated into RNNs for addressing these problems, which transforms them from a conventional type to DRNN. The DRNN remembers long- and short-term temporal dependency of target data by defining when to update the associated value of a new unit named the memory cell. The memory cell comprises three gating units: output, update, and forget gates. Every gate receives a separate input afterwards, passing through the LSTM unit, and they are given as follows:

$$f_r = \sigma_s(w_{f,t}^T[a_{t-1}, X_t] + b_{f,t}); \forall t \in \{1,2,\ldots,T\} \tag{2}$$

$$u_r = \sigma_s(w_{u,t}^T[a_{t-1}, X_r] + b_{u,t}); \forall t \in \{1,2,\ldots, T\} \tag{3}$$

$$\mathrm{o}_r = \sigma_s(w_{o,t}^T[a_{t-1}, X_t] + b_{o,t}); \forall t \in \{1,2,\ldots, T\}. \tag{4}$$

By using the BP model, the weighting vectors $W_f$, $W_u$, $W_o$, and $W_c$, along with bias vectors $b_f$, $b_u$, $b_o$, and $b_c$ are learned. An accurate value for the weighting factor $w_{j,\mathrm{m}}^l$, at $k$th training step and between the output of the next layer $m$ and the inputs feeding neuron $j$ in layer $l$, are updated by means of stochastic gradient descent:

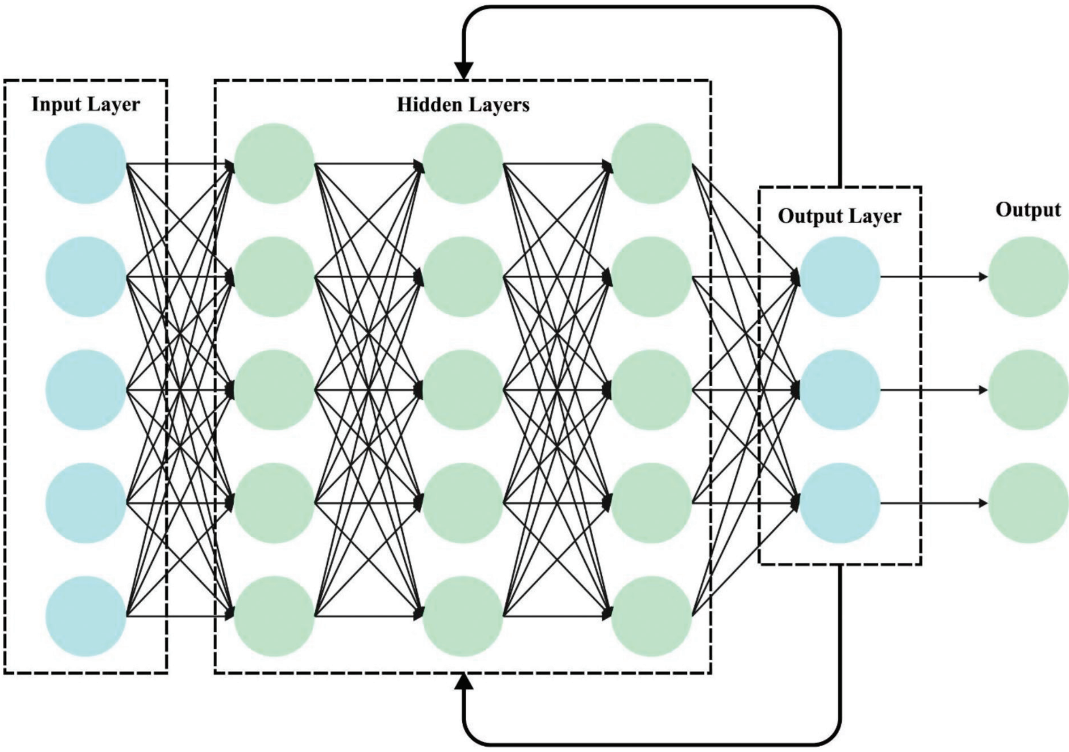


**Figure 2:** RNN architecture.

$$(W^{1}_{j,\mathrm{m}})_{\mathrm{k}} = (w^{l}_{j,\mathrm{m}})_{k-1} - \beta \frac{\partial CE}{\partial (w^{l}_{j,m})_{\mathrm{k}-1}}; \forall j \in \{1,2,\ldots,N_l\}, \forall m$$

$$\in \{1,2,\ldots,N_{l-1}\}, \forall l \in \Gamma,\ \forall k \in \{1,2,\ldots,N_c\}. \tag{5}$$

The last term represents the partial derivative of the parameters controlled by the learning rate $\beta$. The cross entropy loss function with respect to the target value is exploited to evaluate the accuracy of the model.

$$CE = \frac{1}{T}\sum\nolimits_{t=1}^{T}\sum\nolimits_{c=1}^{N_c} d^{a}_{t\,c}\ \log\left(P_{d_{t,c}}\right) \tag{6}$$

In Eq. (6), $P_{d_{t,c}}$ shows the probability estimate output by the network for the training example. $d^{a}_{t,c}$ is equivalent to 1 if the target class for $t$th instance is $c$, or else it is 0. $d^{a}_{t,c}$ and $d_{t,c}$ denote the actual and predicted values of the target class $c$, correspondingly.

## Hyperparameter tuning using the MFO algorithm

Finally, the MFO algorithm is utilized to fine tune the hyperparameter values related to the DRNN method. MFO algorithm is dependent upon the mating way of the mayfly (MF) and the flight performance that integrates the evolutionary algorithms and optimum features of SI optimizer techniques (Zghoul et al., 2023). In MA, two population sets can be arbitrarily created to represent the female and male mayflies (FMFs and MMFs). The location of all the MFs in the problem space defines the candidate solution to optimizer issue. The MFs' position is provided by $n$-dimensional vector = $(x_1, x_2, \ldots, x_n)$, whereas the main function was calculated for evaluating all the MF performances. All the MFs' positions were upgraded utilizing their velocity provided by vector = $(v_1, v_2, \ldots, v_n)$, and flying routes. The MF flying route was defined by better individual flying skills of every MF Pest and better swarm social flying experiences $g_{best}$.

An individual in the MA upgrades their place in the problem space dependent upon its present positions $p_{i^t}$ and velocity $v_{i^t}$ for all the iterations utilized in Eq. (7).

$$P_i^{t+1} = P_i^{t} + V_i^{t+1}. \tag{7}$$

During the MFO algorithm, an MF's velocity is described as the change in their place. The flight route of an MF was controlled by a difficult interaction of their individual and the group's flying encounters. All the MFs alter their flight route for obtaining nearby their optimum position ($p_{best}$). And the optimum position developed by some MFs from the swarm ($g_{best}$). During all the iterations, the male MFs endure

**Table 1:** Details on database.

| Class | Label | No. of samples |
|---|---|---|
| Sitting | C-1 | 1777 |
| Standing | C-2 | 1906 |
| Lying | C-3 | 1944 |
| Walking | C-4 | 1722 |
| Walking upstairs | C-5 | 1544 |
| Walking downstairs | C-6 | 1406 |
| Total number of samples | | 10,299 |

the exploring procedure in swarms. The position of MMFs is upgraded utilizing Eq. (8).

$$X_i^{t+1=x_i^t+v_i^{t+1}}, \quad (8)$$

in which $x_{i^t}$ stands for the present position of MMFs at time step $t$, and $v_{i^{t+1}}$ denotes the MF's velocity. The MMFs fly some meters above the surface of the water and progress at maximum speeds. The velocity of MMFs can be computed using Eq. (9).

$$v_{ij}^{t+1} = v_{ij}^t + a_1 e^{-\beta r_p^2}(p_{best_{ij}} - X_{ij}^t) + a_2 e^{-\beta r_g^2}(g_{best_{ij}} - X_{ij}^t), \quad (9)$$

where $r_g$ and $r_p$ denote the Cartesian distance for global and personal positions, correspondingly; $a_1$ and $a_2$ stand for the personal and global positive coefficients, correspondingly; $\beta$ implies the visibility coefficient, Pest refers to the optimum position of MFs, and $g_{best}$ indicates the optimal global position of MFs.

The velocity of optimum MMFs from the present iteration was upgraded using Eq. (10).

$$V_{ij}^{t+1} = v_{ij}^t + d \times r, \quad (10)$$

in which $d$ denotes the parameter of nuptial dance and $r$ signifies the arbitrary number from the range of 1 and 1. The FMFs' velocity is dependent upon the distance between the females and males. FMFs fly to MMFs for mating. The position of FMFs was upgraded using Eq. (11).

$$\gamma_i^{t+1} = y_i^t + v_i^{t+1}, \quad (11)$$

where $y_{i^t}$ represents the present position of FMF at time step $t$. During the MA, an optimum female. The velocity of females is computed using Eq. (12).

$$v_{ij}^{t+1} = \begin{cases} v_{ij}^t + a_2 e^{-\beta r_{mf}^2}(x_{ij}^t - y_{ij}^t) if\ f(y_i) \geq f(X_i) \\ v_{ij}^t + fl * r \qquad if\ f(y_i) \leq f(X_i) \end{cases}, \quad (12)$$

in which $v_{ij}^t$ signifies the FMFs' velocity from the dimensional $j$ at time $t$, $y_{ij}^t$ represents the position of FMFs from the dimensional $j$ at time $t$, $x_{ij}^t$ stands for the position of MMFs in $j$ at time $t$, $\beta$ and $a_2$ denote the visibility coefficient, and positive constant, correspondingly, $r_{mf}$ stands for the Cartesian distance among FMFs and MMFs, and $f_1$ and $r$ indicate the random walk coefficient and an arbitrary number from the range, correspondingly. In MA, all the couples of MFs create two offspring. One is randomly included in the female population, and the other is in the male population. The two offspring can be created and then mated, as depicted in Eqs. (13) and (14).

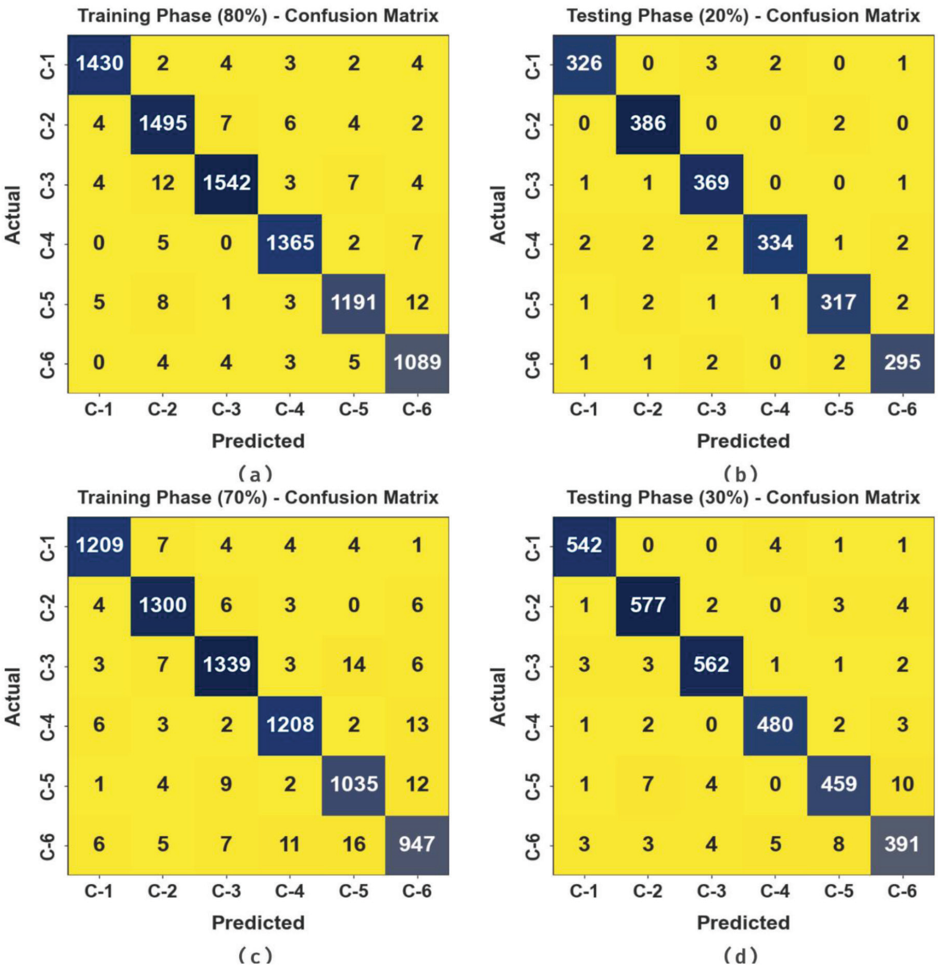


**Figure 3:** Confusion matrices of the ODRNN-HAR system: (a, b) 80:20 TRP/TSP and (c, d) 70:30 TRP/TSP. Abbreviation: ODRNN-HAR, Optimal Deep Recurrent Neural Networks for Human Activity Recognition.

$$Offspring_1 = L \times male + (1-L) \times female \quad (13)$$

$$Offspring_2 = L \times female + (1-L) \times male, \quad (14)$$

where $L$ denotes the random number with Gaussian distribution.

The MFO approach develops a fitness function (FF) to get higher classifier performances. It resolves a positive value that represents the candidate outcomes best outcomes. Here, the minimized classifier rate of errors is FF, defined in Eq. (15).

$$fitness\,(x_i) = ClassifierErrorRate\,(x_i)$$

$$= \frac{number\ of\ misclassified\ samples}{Total\ number\ of\ samples} * 100 \quad (15)$$

## RESULTS AND DISCUSSION

In this section, the experimental validation of the ODRNN-HAR method is tested on the UCI-HAR dataset (UCI-HAR dataset). It has 10,299 samples with six classes, as described in Table 1.

The HAR results of the ODRNN-HAR method are illustrated in the form of confusion matrix in Figure 3. The results stated that the ODRNN-HAR technique detects six types of activities accurately.

In Table 2 and Figure 4, comprehensive HAR results of the ODRNN-HAR technique are reported. The experimental values signified that the ODRNN-HAR technique detects different types of activities proficiently. For example, with 80% of TRP, the ODRNN-HAR approach gains average $accu_y$ of 99.49%, $prec_n$ of 98.42%, $spec_y$ of 99.69%, $F_{score}$ of 98.43%, and MCC of 98.12%. Likewise, with 20% of TSP, the ODRNN-HAR approach gains average $accu_y$ of 99.47%, $prec_n$ of 98.40%, $spec_y$ of 99.68%, $F_{score}$ of 98.37%, and MCC of 98.05%. Then, with 70% of TRP, the ODRNN-HAR algorithm gains average $accu_y$ of 99.21%, $prec_n$ of 97.55%, $spec_y$ of 99.53%, $F_{score}$ of 97.54%, and MCC of 97.07%. Finally, with 30% of TSP, the ODRNN-HAR technique gains average $accu_y$ of 99.15%, $prec_n$ of 97.34%, $spec_y$ of 99.49%, $F_{score}$ of 97.31%, and MCC of 96.80%.

Figure 5 inspects the accuracy of the ODRNN-HAR approach in the training and validation of the test database. The result specified that the ODRNN-HAR technique has greater accuracy values over higher epochs. Moreover, the

**Table 2:** HAR outcome of the ODRNN-HAR system with varying classes and measures.

| Class | $Accu_y$ | $Prec_n$ | $Spec_y$ | $F_{score}$ | MCC |
|---|---|---|---|---|---|
| Training phase (80%) | | | | | |
| Sitting (C-1) | 99.66 | 99.10 | 99.81 | 99.03 | 98.82 |
| Standing (C-2) | 99.34 | 97.97 | 99.54 | 98.23 | 97.82 |
| Lying (C-3) | 99.44 | 98.97 | 99.76 | 98.53 | 98.19 |
| Walking (C-4) | 99.61 | 98.70 | 99.74 | 98.84 | 98.61 |
| Walking upstairs (C-5) | 99.41 | 98.35 | 99.72 | 97.98 | 97.64 |
| Walking downstairs (C-6) | 99.45 | 97.41 | 99.59 | 97.98 | 97.66 |
| Average | 99.49 | 98.42 | 99.69 | 98.43 | 98.12 |
| Testing phase (20%) | | | | | |
| Sitting (C-1) | 99.47 | 98.49 | 99.71 | 98.34 | 98.02 |
| Standing (C-2) | 99.61 | 98.47 | 99.64 | 98.97 | 98.74 |
| Lying (C-3) | 99.47 | 97.88 | 99.53 | 98.53 | 98.21 |
| Walking (C-4) | 99.42 | 99.11 | 99.83 | 98.24 | 97.89 |
| Walking upstairs (C-5) | 99.42 | 98.45 | 99.71 | 98.14 | 97.80 |
| Walking downstairs (C-6) | 99.42 | 98.01 | 99.66 | 98.01 | 97.67 |
| Average | 99.47 | 98.40 | 99.68 | 98.37 | 98.05 |
| Training phase (70%) | | | | | |
| Sitting (C-1) | 99.45 | 98.37 | 99.67 | 98.37 | 98.04 |
| Standing (C-2) | 99.38 | 98.04 | 99.56 | 98.30 | 97.92 |
| Lying (C-3) | 99.15 | 97.95 | 99.52 | 97.77 | 97.25 |
| Walking (C-4) | 99.32 | 98.13 | 99.62 | 98.01 | 97.60 |
| Walking upstairs (C-5) | 99.11 | 96.64 | 99.41 | 97.00 | 96.48 |
| Walking downstairs (C-6) | 98.85 | 96.14 | 99.39 | 95.80 | 95.14 |
| Average | 99.21 | 97.55 | 99.53 | 97.54 | 97.07 |
| Testing phase (30%) | | | | | |
| Sitting (C-1) | 99.51 | 98.37 | 99.65 | 98.64 | 98.34 |
| Standing (C-2) | 99.19 | 97.47 | 99.40 | 97.88 | 97.38 |
| Lying (C-3) | 99.35 | 98.25 | 99.60 | 98.25 | 97.85 |
| Walking (C-4) | 99.42 | 97.96 | 99.62 | 98.16 | 97.81 |
| Walking upstairs (C-5) | 98.80 | 96.84 | 99.43 | 96.13 | 95.42 |
| Walking downstairs (C-6) | 98.61 | 95.13 | 99.25 | 94.79 | 93.99 |
| Average | 99.15 | 97.34 | 99.49 | 97.31 | 96.80 |

Abbreviation: HAR, human activity recognition.

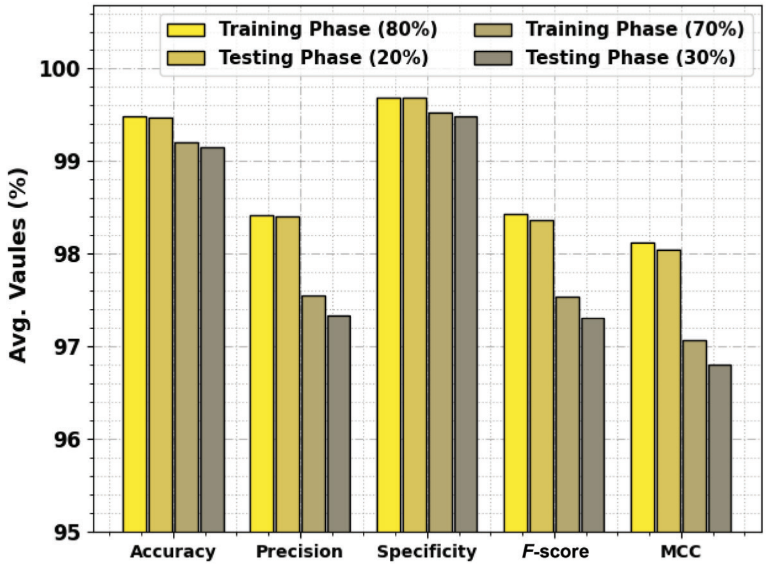


**Figure 4:** Average outcome of the ODRNN-HAR system with varying measures. Abbreviation: ODRNN-HAR, Optimal Deep Recurrent Neural Networks for Human Activity Recognition.

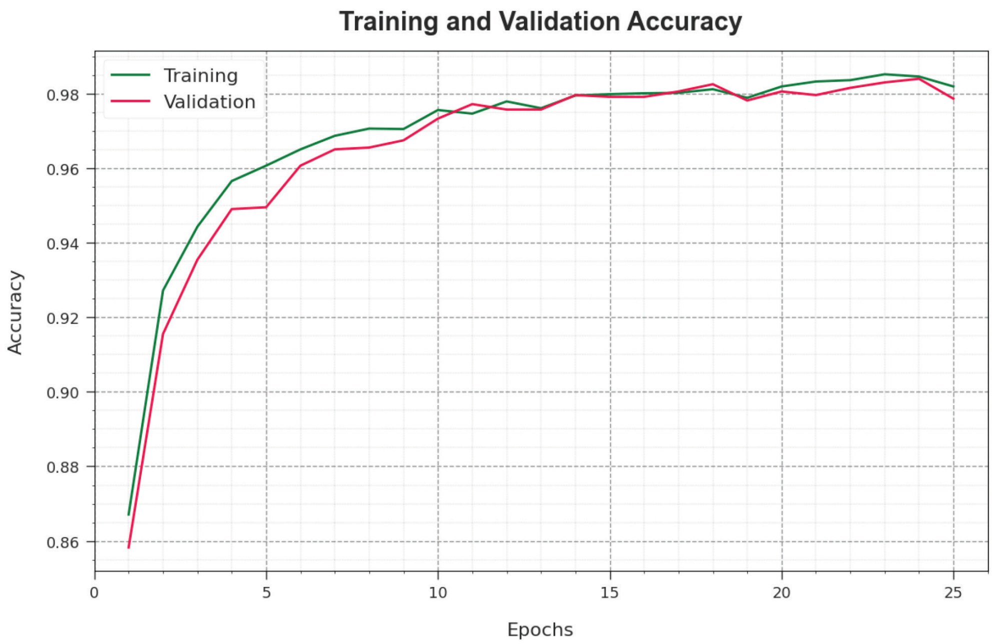


**Figure 5:** Accuracy curve of the ODRNN-HAR system. Abbreviation: ODRNN-HAR, Optimal Deep Recurrent Neural Networks for Human Activity Recognition.

increasing validation accuracy over training accuracy portrayed that the ODRNN-HAR method learned productively on the test database.

The loss analysis of the ODRNN-HAR technique at the time of training and validation is shown on the test database in Figure 6. The results show that the ODRNN-HAR algorithm reaches closer value of training and validation loss. The ODRNN-HAR approach learns productively on the test database.

A brief precision-recall (PR) curve of the ODRNN-HAR technique is given on the test database in Figure 7. The results state that the ODRNN-HAR approach increases PR values. In addition, it is noticeable that the ODRNN-HAR technique can reach higher PR values in all classes.

In Figure 8, an ROC study of the ODRNN-HAR approach is revealed on the test database. The figure describes the ODRNN-HAR methodology to improve the ROC values. Besides, the ODRNN-HAR approach can extend enhanced ROC values to all classes.

A brief comparative assessment of the ODRNN-HAR technique with current approaches is made in Table 3 and Figure 9 (Duhayyim, 2023). Based on $accu_y$, the ODRNN-HAR technique reaches higher $accu_y$ of 99.49%, while the ODRNN-HAR, IPODTL-HAR, RF, NNN, SVM, ANN,

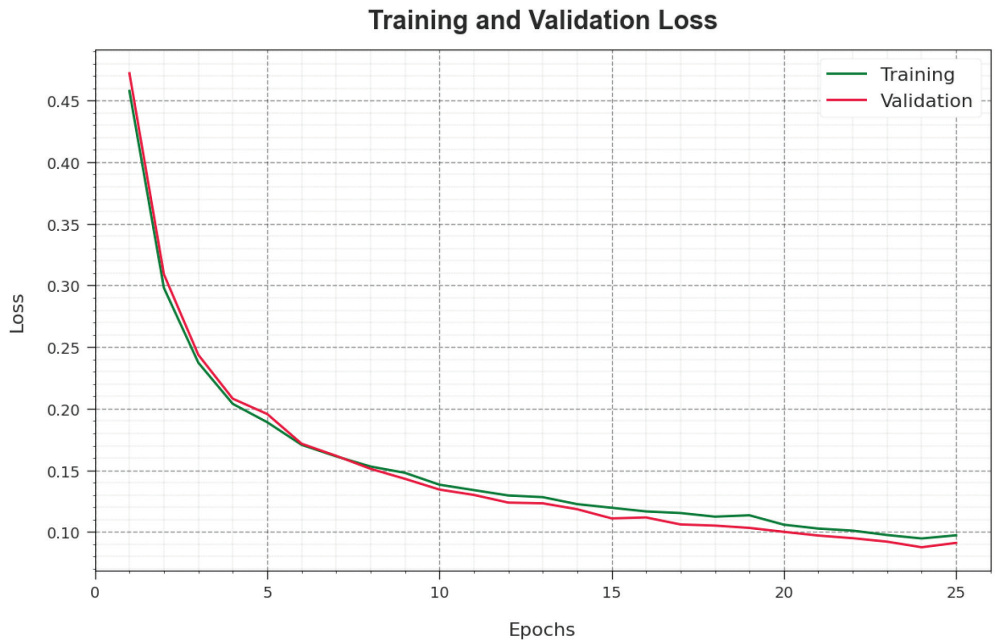


**Figure 6:** Loss curve of the ODRNN-HAR system. Abbreviation: ODRNN-HAR, Optimal Deep Recurrent Neural Networks for Human Activity Recognition.

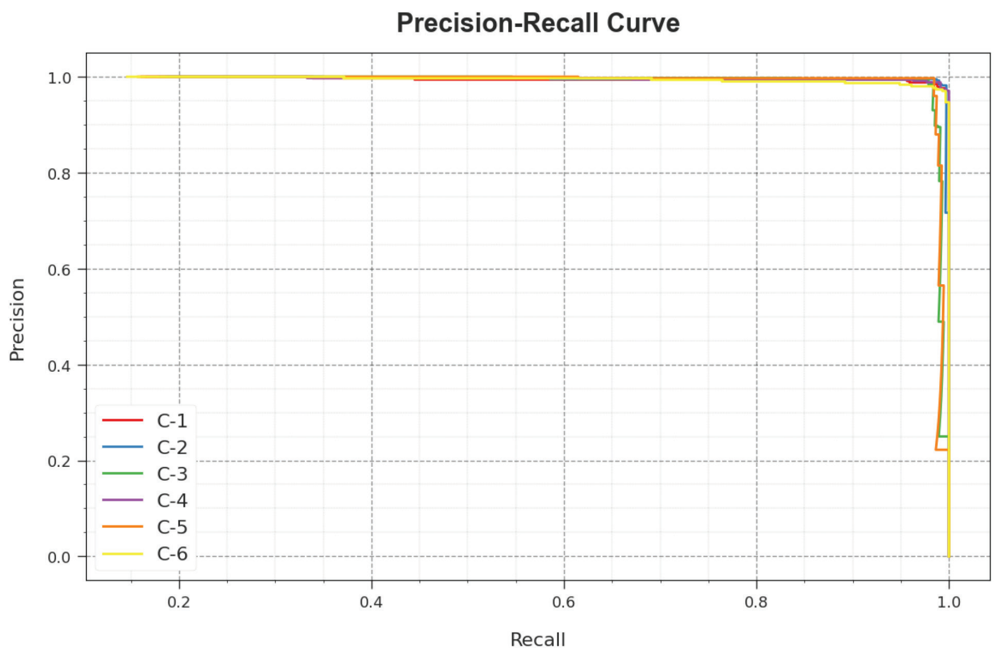


**Figure 7:** PR curve of the ODRNN-HAR system. Abbreviation: ODRNN-HAR, Optimal Deep Recurrent Neural Networks for Human Activity Recognition.

and LSTM models yield lower $accu_y$ of 99.10, 86.18, 87.50, 88.81, 91.83, and 93.97%, respectively. Eventually, based on $prec_n$, the ODRNN-HAR technique reaches higher $prec_n$ of 98.42%, while the ODRNN-HAR, IPODTL-HAR, RF, NNN, SVM, ANN, and LSTM models yield lower $prec_n$ of 97.44, 82.70, 85.86, 88.86, 88.56, and 91.82%, respectively. Similarly, based on $spec_y$, the ODRNN-HAR approach reaches higher $spec_y$ of 99.69%, while the ODRNN-HAR, IPODTL-HAR, RF, NNN, SVM, ANN, and LSTM models yield lower $spec_y$ of 99.09, 80.96, 82.76, 87.44, 92.20, and 94% correspondingly.

Therefore, the ODRNN-HAR technique exhibited improved activity recognition performance over other models.

# CONCLUSION

In this study, an automated HAR detection using the ODRNN-HAR method has been developed in IoT environment. The major intention of the ODRNN-HAR technique lies in the automated recognition and classification of various

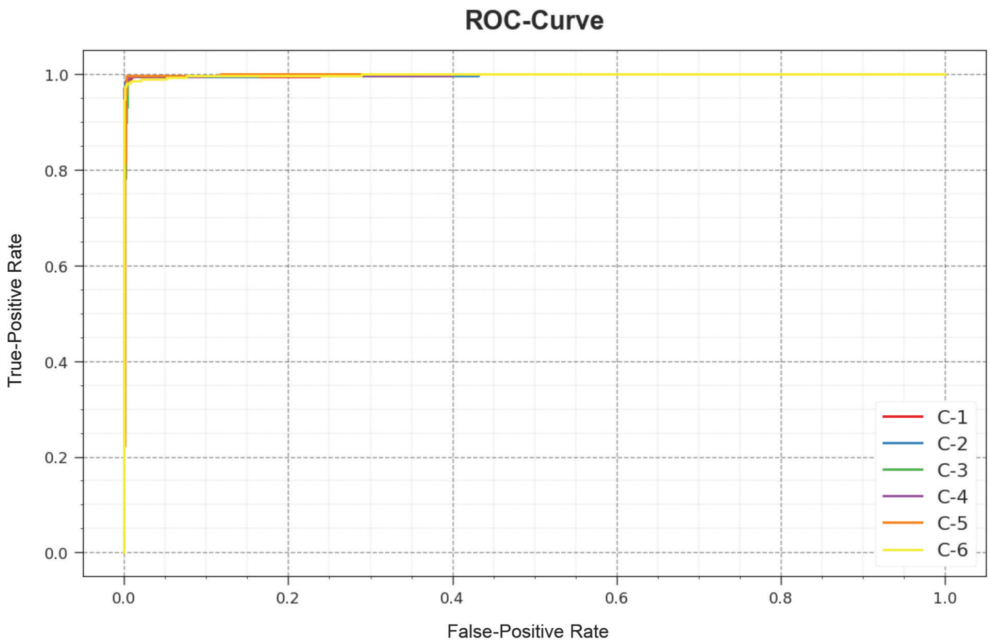


**Figure 8:** ROC curve of the ODRNN-HAR system. Abbreviation: ODRNN-HAR, Optimal Deep Recurrent Neural Networks for Human Activity Recognition.

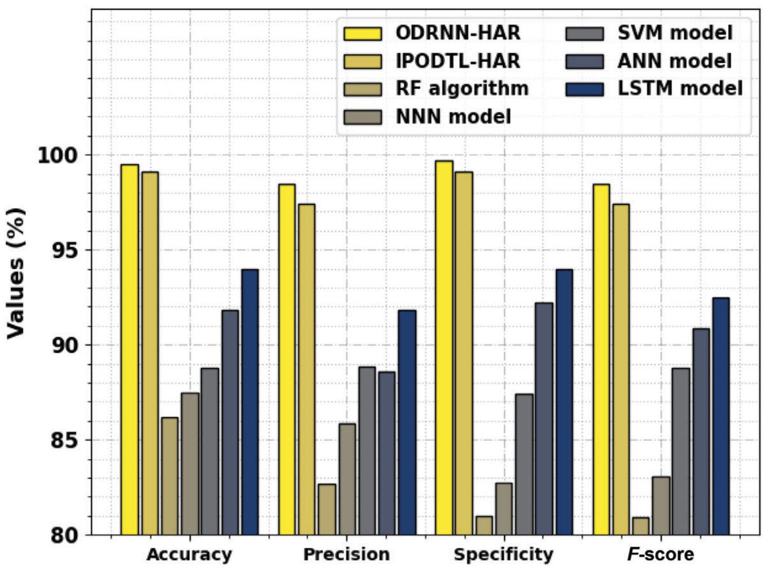


**Figure 9:** Comparative outcome of the ODRNN-HAR approach with existing methods. Abbreviation: ODRNN-HAR, Optimal Deep Recurrent Neural Networks for Human Activity Recognition.

**Table 3:** Comparative outcome of the ODRNN-HAR method with existing methods.

| Methods | $Accu_y$ | $Prec_n$ | $Spec_y$ | *F*-score |
|---|---|---|---|---|
| ODRNN-HAR | 99.49 | 98.42 | 99.69 | 98.43 |
| IPODTL-HAR | 99.10 | 97.44 | 99.09 | 97.39 |
| RF algorithm | 86.18 | 82.70 | 80.96 | 80.94 |
| NNN model | 87.50 | 85.86 | 82.76 | 83.06 |
| SVM model | 88.81 | 88.86 | 87.44 | 88.80 |
| ANN model | 91.83 | 88.56 | 92.20 | 90.85 |
| LSTM model | 93.97 | 91.82 | 94.00 | 92.50 |

kinds of human activities in IoT environment. Several subprocesses are involved in the presented MER-ODLADT technique, namely data preprocessing, DRNN-based activity recognition, and MFO-based hyperparameter tuning. For effectual recognition of human activities, the ODRNN-HAR technique uses the DRNN model. At the final stage, the optimal hyperparameter adjustment of the DRNN model takes place using the MFO algorithm. The result analysis of the ODRNN-HAR algorithm takes place on benchmark HAR dataset, and the outcomes are examined in terms of different measures. The comprehensive simulation results highlighted the improved recognition outcomes of the ODRNN-HAR method in terms of different measures. In future, a multi-modal fusion-based DL approach can be derived to improve the recognition results of the ODRNN-HAR method.

## FUNDING

The authors extend their appreciation to the King Salman Center for Disability Research for funding this work through Research Group no KSRG-2023-114.

## CONFLICTS OF INTEREST

The authors declare no conflicts of interest in association with the present study.

## DATA AVAILABILITY STATEMENT

Data sharing is not applicable to this article as no datasets were generated during the current study.

## REFERENCES

Anagnostis A., Benos L., Tsaopoulos D., Tagarakis A., Tsolakis N. and Bochtis D. (2021). Human activity recognition through recurrent neural networks for human–robot interaction in agriculture. *Appl. Sci.*, 11(5), 2188.

Brishtel I., Krauss S., Chamseddine M., Rambach J.R. and Stricker D. (2023). Driving activity recognition using UWB radar and deep neural networks. *Sensors*, 23(2), 818.

Dahou A., Al-qaness M.A., Abd Elaziz M. and Helmi A. (2022). Human activity recognition in IoHT applications using arithmetic optimization algorithm and deep learning. *Measurement*, 199, 111445.

Duhayyim M.A. (2023). Parameter-tuned deep learning-enabled activity recognition for disabled people. *Comput. Mater. Contin.*, 75(3), 6587-6603.

Eskandari A., Aghaei M., Milimonfared J. and Nedaei A. (2023). A weighted ensemble learning-based autonomous fault diagnosis method for photovoltaic systems using genetic algorithm. *Int. J. Electr. Power Energy Syst.*, 144, 108591.

Gumaei A., Hassan M.M., Alelaiwi A. and Alsalman H. (2019). A hybrid deep learning model for human activity recognition using multimodal body sensing data. *IEEE Access*, 7, 99152-99160.

Islam M.S., Jannat M.K.A., Hossain M.N., Kim W.S., Lee S.W. and Yang S.H. (2023). STC-NLSTMNet: an improved human activity recognition method using convolutional neural network with NLSTM from WiFi CSI. *Sensors*, 23(1), 356.

Lattanzi E., Donati M. and Freschi V. (2022). Exploring artificial neural networks efficiency in tiny wearable devices for human activity recognition. *Sensors*, 22(7), 2637.

Li B., Cui W., Wang W., Zhang L., Chen Z. and Wu M. (2021). Two-stream convolution augmented transformer for human activity recognition. In: *Proceedings of the AAAI Conference on Artificial Intelligence*, 2-9 February 2021; vol. 35(1); pp. 286-293.

Li H., Shrestha A., Heidari H., Le Kernec J. and Fioranelli F. (2019). Bi-LSTM network for multimodal continuous human activity recognition and fall detection. *IEEE Sens. J.*, 20(3), 1191-1201.

Mekruksavanich S., Jitpattanakul A., Youplao P. and Yupapin P. (2020). Enhanced hand-oriented activity recognition based on smartwatch sensor data using LSTMs. *Symmetry*, 12(9),1570.

Park H., Kim N., Lee G.H. and Choi J.K. (2023). MultiCNN-FilterLSTM: resource-efficient sensor-based human activity recognition in IoT applications. *Future Gener. Comp. Syst.*, 139, 196-209.

Qian H., Pan S.J. and Miao C. (2021). Latent independent excitation for generalizable sensor-based cross-person activity recognition. In: *Proceedings of the AAAI Conference on Artificial Intelligence*, 2-9 February 2021; vol. 35(13); pp. 11921-11929.

Rashid K.M. and Louis J. (2019). Times-series data augmentation and deep learning for construction equipment activity recognition. *Adv. Eng. Inform.*, 42, 100944.

Shan C.Y., Han P.Y. and Yin O.S. (2020). Deep analysis for smartphone-based human activity recognition. In: *2020 8th International Conference on Information and Communication Technology (ICoICT)*. IEEE, Malaysia, 21-23 October 2020; pp. 1-5.

Taheri S., Ahmadi A., Mohammadi-Ivatloo B. and Asadi S. (2021). Fault detection diagnostic for HVAC systems via deep learning algorithms. *Energy Build.*, 250, 111275.

Tang C.I., Perez-Pozuelo I., Spathis D., Brage S., Wareham N. and Mascolo C. (2021). Selfhar: improving human activity recognition through self-training with unlabeled data. arXiv, arXiv:2102.06073.

UCI-HAR Dataset. https://archive.ics.uci.edu/ml/datasets/human+activity+recognition+using+smartphones.

Ullah M., Ullah H., Khan S.D. and Cheikh F.A. (2019). Stacked LSTM network for human activity recognition using smartphone data. In: *2019 8th European Workshop on Visual Information Processing (EUVIP)*. IEEE, Roma, Italy, 28-31 October 2019; pp. 175-180.

Xia K., Huang J. and Wang H. (2020). LSTM-CNN architecture for human activity recognition. *IEEE Access*, 8, 56855-56866.

Xu H., Li J., Yuan H., Liu Q., Fan S., Li T. and Sun X. (2020). Human activity recognition based on Gramian angular field and deep convolutional neural network. *IEEE Access*, 8, 199393-199405.

Zghoul F.N., Alteehi H. and Abuelrub A. (2023). A mayfly-based approach for CMOS inverter design with symmetrical switching. *Algorithms*, 16(5), 237.

Zhang J., Zi L., Hou Y., Wang M., Jiang W. and Deng D. (2020). A deep learning-based approach to enable action recognition for construction equipment. *Adv. Civ. Eng.*, 2020, 1-14.